NOTES AND CORRESPONDENCE

Potential Vorticity, Easterly Waves, and Eastern Pacific Tropical Cyclogenesis

JOHN MOLINARI, DAVID KNIGHT, MICHAEL DICKINSON, DAVID VOLLARO, AND STEVEN SKUBIS

Department of Earth and Atmospheric Science, State University of New York at Albany, Albany, New York

12 January 1996 and 12 August 1996

ABSTRACT

A significant sign reversal in the meridional potential vorticity gradient was found during the summer of 1991 on the 310-K isentropic surface (near 700 mb) over the Caribbean Sea. The Charney–Stern necessary condition for instability of the mean flow is met in this region. It is speculated that the sign reversal permits either invigoration of African waves or actual generation of easterly waves in the Caribbean.

During the same season, a correlation existed between the strength of the negative potential vorticity gradient in the Caribbean and subsequent cyclogenesis in the eastern Pacific. The meridional PV gradient, convective heating measured by outgoing longwave radiation data, and eastern Pacific cyclogenesis all varied on the timescale of the Madden–Julian oscillation (MJO). It is hypothesized that upstream wave growth in the dynamically unstable region provides the connection between the MJO (or any other convective forcing) and the associated enhanced downstream tropical cyclogenesis.

1. Introduction

It is frequently stated that tropical cyclogenesis in the eastern Pacific Ocean occurs in association with easterly waves that have propagated from Africa across the Atlantic and Caribbean and into the eastern Pacific (Avila 1991; Avila and Pasch 1992). The mechanism for the source of these waves was proposed by Burpee (1972). He showed that the meridional gradient of potential vorticity changed sign over Africa near 700 mb during the warm season. This sign reversal satisifies a necessary condition for instability of the mean flow (Charney and Stern 1962). Waves that develop in this potentially unstable region are typically labeled African waves. Shapiro (1986) showed that strong African waves can maintain their structure while propagating across the Atlantic Ocean and into the eastern Pacific. Carlson (1969) noted that more typically African waves weakened over the central Atlantic, but most could be tracked to the Caribbean. These papers provide support for the extended propagation of African waves from their source region.

The difficulty with the above reasoning has been noted by D. Raymond (1996, personal communication): localized easterly waves can be characterized as Rossby wave packets, which are dispersive. In the absence of convection, a local disturbance would weaken and lose its structure before reaching the eastern Pacific. The disturbances in Shapiro's (1986) study contained substantial convection, but typically convection is not maintained in the disturbances over the cool central Atlantic (Carlson 1969). It is not obvious how African waves could reach the Pacific under such circumstances. This uncertainty arises in part because, with the exception of Shapiro (1977), the background state in which these disturbances traverse the Atlantic has not been investigated.

A related question concerns fluctuations in eastern Pacific tropical cyclogenesis, which often displays active and inactive periods. If African waves are indeed associated with such cyclogenesis, it might be expected that corresponding active and inactive periods would occur upstream over Africa at a previous time. Alternatively, such fluctuations could relate to changes in the environment for African waves as they traverse the Atlantic.

The 1991 eastern Pacific hurricane season provides an excellent opportunity to address these issues. First, although 73 wave disturbances crossed the African coast between May and November (about one every three days), the disturbances were difficult to track across the Atlantic in either the wind field or the cloud field throughout the season (Avila and Pasch 1992). Nevertheless, Avila and Pasch (1992) were able to associate each eastern Pacific tropical cyclone with a synoptic-scale easterly wave from Africa. The 1991 hurricane season is of further interest because it contains striking

Corresponding author address: Dr. John Molinari, Department of Earth and Atmospheric Science, SUNY at Albany, Earth Science 351, Albany, NY 12222.
E-mail: molinari@atmos.albany.edu

fluctuations in the frequency of tropical cyclogenesis, with several distinct active and inactive periods.

This note will focus on the characteristics of the zonally nonuniform background state between Africa and the eastern Pacific during the 1991 hurricane season. In this way the work will have conceptual similarities to that of Shapiro (1977, 1980). The methods and proposed mechanism differ, however, and it is eastern Pacific rather than Atlantic tropical cyclogenesis that is of interest here. Time-averaged potential vorticity will provide the basis for this study. The goal is to describe a framework that allows the role of African waves in the eastern Pacific to be addressed, and to attempt to understand active and inactive periods in terms of variations in the background state.

2. Data sources and calculation methods

a. ECMWF gridded analyses

Several calculations make use of uninitialized gridded analyses on pressure surfaces from the European Centre for Medium-Range Weather Forecasts (ECMWF). Most of the analyses were obtained directly from ECMWF on a 1.125° latitude–longitude grid and at 12 pressure levels. The remainder were generated in the identical manner as ECMWF from spectral coefficients stored at the National Center for Atmospheric Research. The regions of interest in this study, the subtropical Atlantic and eastern Pacific Oceans, are not areas of substantial data coverage. Nevertheless, a number of studies have made successful use of the ECMWF analyses in data-sparse regions of the Tropics and subtropics. Three such studies will be discussed here. The first is by Reed et al. (1988), who examined ECMWF global model 48-h forecasts of easterly waves. Because the four-dimensional data assimilation process used by ECMWF makes use of a model forecast as a first guess, forecast accuracy will contribute to analysis accuracy. Reed et al. (1988) found that the model possessed ''considerable skill'' in wave prediction over west Africa, the far eastern Atlantic, and the Caribbean. There also was evidence of skill in the central Atlantic, where most but not all easterly waves trackable via satellite were present in the forecasts. Reed et al. (1988) also provided evidence that the ECMWF model reproduced rapidly growing easterly waves without the benefit of data. This likely reflects the presence of an accurate background state in which the wave can grow.

The second paper of interest is by Liebmann and Hendon (1990). They filtered ECWMF analyses to get composite Rossby–gravity waves over the tropical Atlantic and Pacific Oceans. Not only was the wave structure remarkably like the idealized Rossby–gravity wave solution, but independently derived outgoing longwave radiation showed deep convection in the part of the wave where it would be expected (Hendon 1986). The evidence suggests that equatorial synoptic-scale waves are adequately represented in the ECMWF analyses even over midocean regions.

The third relevant paper is by Boer (1995), who examined several years of global wavenumber 1 velocity potential field at 200 mb averaged over 15°S–15°N. A remarkably coherent Madden–Julian oscillation that sometimes circled the globe twice was reproduced by the ECMWF analyses. In addition, the oscillation was well maintained in 48-h forecasts. This suggests that even if *no* data were present over several 6-h update cycles, the four-dimensional data analysis/assimilation process should be able to carry such an oscillation forward in time and space.

The above papers show that ECMWF gridded analyses have reasonable skill on the synoptic and planetary scale in the Tropics and subtropics. Nevertheless, a cautionary comment is needed. In the absence of reliable data sources, detailed calculations for individual disturbances of, for instance, barotropic and baroclinic energy exchanges, might give erratic results. The ECMWF analyses are neither pure numerical simulations nor pure objective analyses, and structural details over ocean likely depend upon the chance presence of data at a given time. Instead, the emphasis in this paper will be on examination of time-averaged or low-pass filtered fields, in which the confidence level should be high.

Outgoing longwave radiation (OLR) data has also been obtained from the National Center for Atmospheric Research. This data was produced in a manner similar to that of Gruber and Krueger (1984), but using *NOAA-12* and *NOAA-14* satellites. Because these satellites are polar orbiting, the representative local time varies with location. This problem has been minimized by examining only low-pass filtered OLR, which eliminates the diurnal cycle (see section 2c).

b. Eastern Pacific hurricanes in 1991

For the purposes of this paper, ''seasonal mean'' will refer to the average between 0000 UTC 15 June and 1200 UTC 30 September 1991. This was defined to encompass the major periods of active tropical cyclogenesis while minimizing the impact of seasonal changes on the mean fields. Information on tropical cyclone track and origin was obtained from the paper by Rappaport and Mayfield (1992). Data for eastern Pacific tropical depressions 5 and 10 was obtained from the National Hurricane Center (R. Pasch 1994, personal communication).

The first depression of the season occurred in mid-May and the last in mid-November. These two disturbances are not part of the current study. Four depressions occurred from middle-to-late June, one in mid-July, three in late July–early August, and six in middle-to-late September and early October. The most concentrated active periods thus began in mid-June, early August, and mid-September, about 45 days apart.

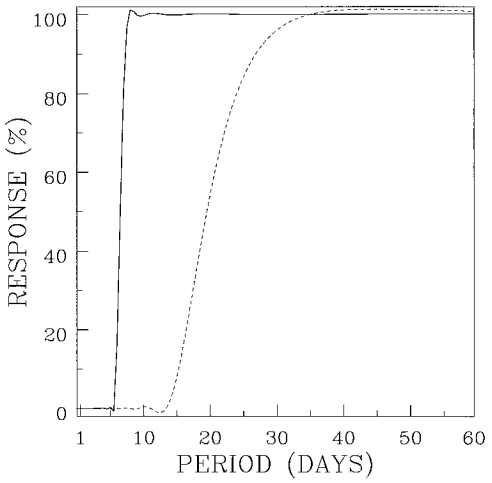

FIG. 1. Response functions for the Lanczos filter with 7-day cutoff (solid) and 20-day cutoff (dashed).

c. Filtering and other calculation methods

A low-pass filter is chosen for this study for two reasons. First, the background state in which the waves propagate is of interest. To isolate this state requires that easterly wave and higher frequencies be filtered out. Second, tropical cyclogenesis varied on long timescales, suggesting that long-period waves might play a role, at least during this particular season.

The choice of a cutoff frequency is difficult. A wide variety of disturbance frequencies have been found in the subtropical Atlantic and eastern Pacific, associated both with Rossby and mixed Rossby–gravity waves. These include diurnal (especially over land), 3–4 day (Nitta and Takabayu 1985), 5–7 day (Nitta and Takabayu 1985), 13–15 day (Krishnamurti et al. 1975), 15–25 day (Nakazawa 1986), and 30–60 day (Madden and Julian 1994). A variety of filter cutoffs were examined. For brevity, only two will be shown: a 20-day cutoff, referred to as the low-pass filter, and a 7-day cutoff, provided for comparison.

Each field was filtered in time at each grid point using a Lanczos filter (Lanczos 1956; Duchon 1979). To sharpen the response, 121 points (60 days) were used on each side of the given time. The resulting response functions for the 20- and 7-day cutoff filters are shown in Fig. 1. It is apparent that for the low-pass filter any oscillations of period below 16 days are largely removed, while periods longer than 24 days are largely retained.

Seasonal means of unfiltered fields will also be calculated. Of particular interest will be the hydrostatic Ertel potential vorticity on isentropic surfaces, given by

$$q = g\sigma^{-1}(\zeta_\theta + f), \tag{1}$$

where $\sigma = -\partial p/\partial\theta$ and ζ_θ represents the vertical component of relative vorticity computed on an isentropic surface. Following Molinari et al. (1995), all fields were linearly interpolated to isentropic surfaces, and q was computed directly on these surfaces. Time averages were determined by the mean PV rather than PV of the mean fields, although the results of the two measures were almost identical.

PV anomaly fields were defined by $q - gf/\langle\sigma\rangle$, where the angle brackets represent a combined area and time average at each level. This represents the departure of PV from a background value dependent upon f and area-averaged stability.

3. Potential vorticity

a. Time-averaged structure

Figure 2 shows the seasonal-mean Ertel potential vorticity on the 310-K isentropic surface. This surface lies between 725 and 825 mb over the Northern Hemisphere subtropical oceans, and extends to near the ground over

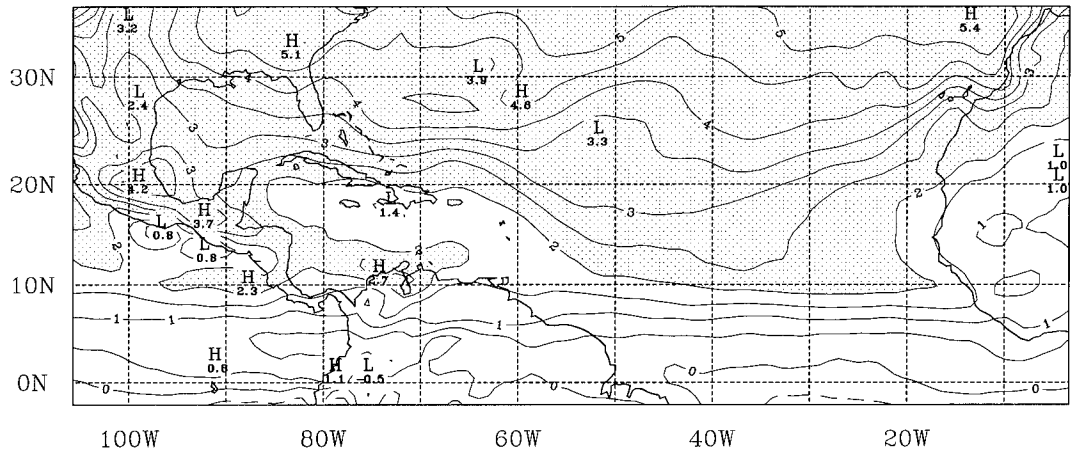

FIG. 2. Seasonal mean potential vorticity for 1991 (15 June–30 September) on the 310-K isentropic surface. Units are 10^{-7} m^2 K s^{-1} kg^{-1} with an increment of 0.5×10^{-7}. Values greater than 2×10^{-7} are shaded.

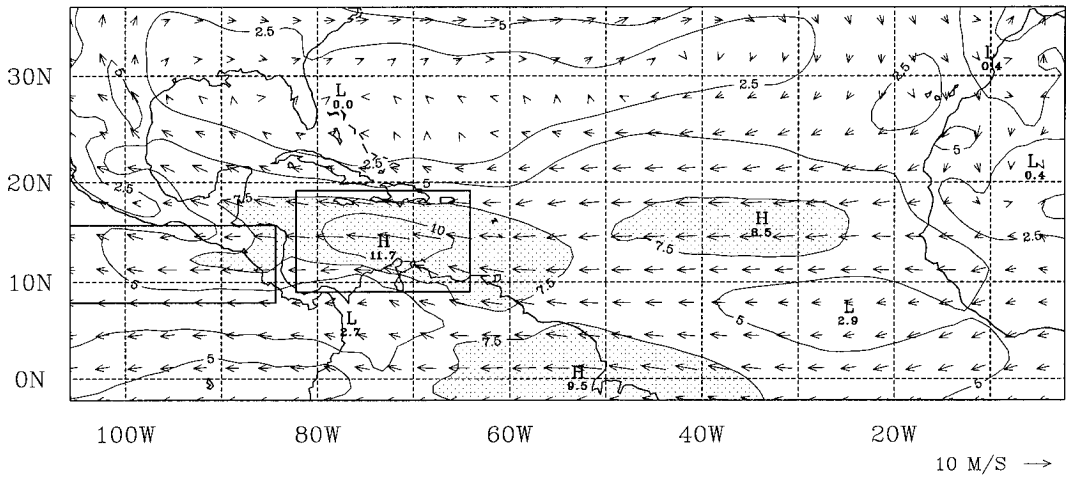

FIG. 3. Seasonal mean wind vectors and isotachs at 310 K. The isotach increment is 2.5 m s^{-1}, and values greater than 7.5 m s^{-1} are shaded. The boxes represent regions to be used for calculation of potential vorticity sign reversals (see section 4).

Africa. In the subtropics, three regions exist in which time-averaged PV decreases northward. Each of these is bounded to the north and south by latitudes where the meridional PV gradient (q_y) changes sign. The strongest of these potentially unstable mean flows is in the Caribbean Sea between the South American coast and Hispaniola. A second smaller region exists over the eastern Pacific just west of Central America. A marginally unstable region is present in west Africa and the eastern Atlantic. The last of these is much stronger at 315 and 320 K (not shown). The q_y sign reversal over Africa is well known based on the work of Burpee (1972), but the extension of this region over the eastern Atlantic, and particularly the existence of the other two regions of sign reversal in the Caribbean and eastern Pacific, has not previously been described.

As noted by Burpee (1972), this PV structure satisfies the Charney–Stern necessary condition for instability of internal jets. An additional necessary condition for instability, the Fjörtoff condition (Fjörtoff 1950; see also Eliassen 1983), requires that the mean zonal current be positively correlated with q_y. Figure 3 shows the seasonal mean wind on the 310-K surface. It is apparent that this additional condition is satisfied in the Caribbean and in a small region of the eastern Pacific, in that regions of $q_y < 0$ each coincide with an easterly jet. The same is true in the eastern Atlantic at 315 K (not shown), where the easterly jet extends much farther eastward over the African continent.

Figure 4 shows a north–south cross section of seasonal mean PV over the Caribbean along 72°W. The shaded regions represent $q_y < 0$. The PV structure in Fig. 4 resembles that of Schubert et al.'s (1991) zonally symmetric model that was produced solely by a 5°C per day diabatic heating maximum at 10°N and 330 K (their Figs. 5 and 8a). Figure 4 is consistent with a strong convective PV source at low levels and sink aloft, which would produce $q_y < 0$ to the north at low levels and to the south at upper levels. The implied convective heating maximum is between 10° and 11°N over South America. This region coincides with Lake Maracaibo, which is well known for its frequent summer thunderstorms that are said to serve as natural lighthouses for fishermen (Codazzi 1841).

The evidence suggests that lower tropospheric PV sources associated with deep convection played a major role in the Caribbean q_y sign reversal. Nevertheless, this cannot be the entire explanation, because negative PV anomalies (not shown; see section 2 for their definition) exist in the northern Caribbean that are as large as the positive anomalies over northern South America. These negative anomalies are not present in Schubert et al.'s (1991) simulations. They are likely associated with three interrelated processes: (i) loss of PV to the ocean over the warm Caribbean, that is, an upward decrease of diabatic heating in the lower troposphere, consistent with a downward ''nonadvective flux'' of PV (Haynes and McIntyre 1987); (ii) extension of the above heating gradient by a field of shallow convection over the Caribbean, which produces warming in the cloud layer and cooling above (Betts 1975; Nitta and Esbenson 1974); and (iii) a likely radiative cooling maximum in the trade wind inversion above the shallow convection. The combination of these three processes will produce heating at low levels and cooling above, consistent with generation of a lower tropospheric negative PV anomaly.

The remaining nonconservative process in the PV equation is proportional to the curl of the friction force. Differential friction in the mean easterly current could be at least partly responsible for the observed positive PV anomaly along the South American coast and neg-

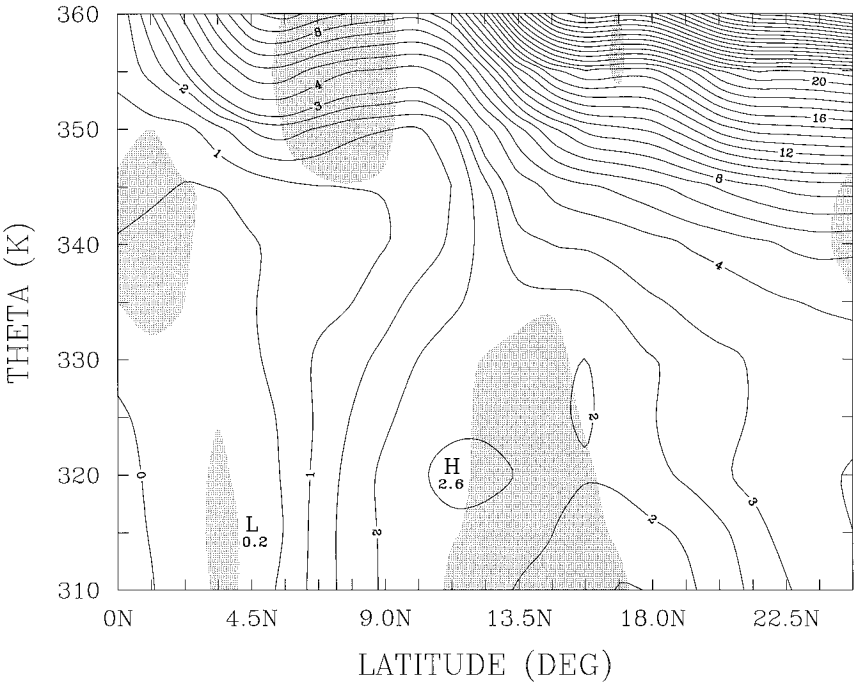

FIG. 4. North–south cross section of seasonal mean PV in the Caribbean at 72°W. The shading indicates regions where $\partial q/\partial y < 0$. Units as in Fig. 3. The plotting increment is 0.5×10^{-7} for values below 3×10^{-7}, and 1×10^{-7} for values above 3×10^{-7}.

ative PV anomaly along the southern Mexican coast, because high terrain exists just inland in both regions.

Regardless of the cause, Figs. 2 and 3 show that the mean flow meets the necessary conditions for unstable growth of waves over a large region in the Caribbean and a smaller region in the eastern Pacific. The possible consequences of this are discussed in the following section.

b. Implications for wave behavior

As waves move from Africa into the eastern Atlantic, a region where the basic state remains strongly unstable at 315 K (and marginally so at 310 K), they would be expected to gain amplitude [see, e.g., the idealized numerical studies of Shapiro (1980) and Thorncroft and Hoskins (1994b)]. Once the waves reach 40°W, the sign reversal of the background PV gradient disappears. In the absence of convection, Rossby wave packets should disperse and thus weaken with time. Such behavior has been observed in a balanced numerical model simulation by D. Raymond (1996, personal communication) and is consistent with the observations of Carlson (1969). As the weakening disturbance reaches the Caribbean, however, the basic state becomes unstable and the disturbance could again grow. Because the Caribbean unstable region has a significant longitudinal extent, growth could occur for approximately 3 days for typical wave speeds of 6–7 m s^{-1}. The consequences for tropical cyclogenesis are (i) African waves reaching the Caribbean could be reinvigorated, making it more likely they would reach the eastern Pacific with sufficient amplitude to initiate tropical cyclones, and thus (ii) fluctuations in eastern Pacific cyclogenesis might be related to prior fluctuations of q_y in the Caribbean.

The eastern Pacific unstable basic state, while small in area, also provides a favorable environment for wave growth. In the following section, the relationship between tropical cyclogenesis in the eastern Pacific and the strength and horizontal scale of the two upstream PV gradient sign reversals will be investigated.

4. Relationship of PV to tropical cyclogenesis during 1991

On the basis of previous arguments, the strength and coverage of the region with $q_y < 0$ will be calculated over the two separate boxes shown in Fig. 3. The boxes were chosen to encompass the regions of sign reversal in the seasonal mean fields. For the reasons given in section 2, only low-pass filtered fields were used for the calculations. In the following discussion, filtered fields will be identified by a tilde.

Two aspects of the negative q_y have dynamical importance: its magnitude, which should relate to the growth rate of a disturbance (see, e.g., Thorncroft and Hoskins 1994a); and its longitudinal scale, which determines the length of time the wave is in the unstable

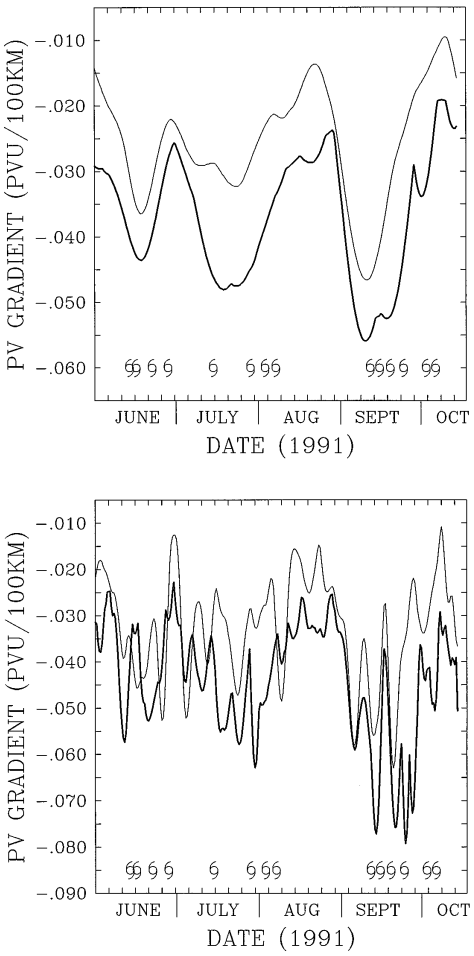

FIG. 5. Time series of two measures of potential vorticity sign reversal over the box in the Caribbean shown in Fig. 3 for (a) 20-day cutoff Lanczos filter; and (b) 7-day cutoff Lanczos filter. Figure 1 gives the respective response functions. The dark lines show min ($\tilde{q}_y$) (tilde indicates filtered values); the light line shows area-weighted mean negative $\tilde{q}_y$ given by Eq. (2) in the text, multiplied by 5 to permit comparison between the two measures of sign reversal. The tropical storm symbols indicate the times of formation of eastern Pacific tropical depressions. Each tickmark on the x axis represents 5 days.

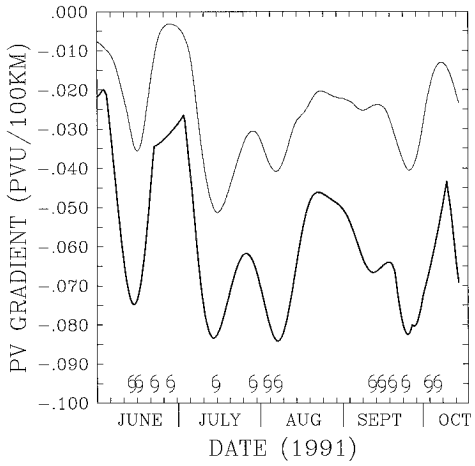

FIG. 6. Same as Fig. 5a, but for the eastern Pacific box shown in Fig. 3.

region. Computation of the average q_y in a box does not provide an effective way of determining the magnitude of the sign reversal, because such an average can include both positive and negative gradients, and their sum tends to blur the results. Instead, two measures of negative meridional PV gradient will be made. The first simply computes the minimum value of $\tilde{q}_y$ in each box. The second incorporates both the magnitude and the areal extent of the negative $\tilde{q}_y$ by calculating the following:

$$\sum \left\{ \frac{\tilde{q}_y \Delta x \Delta y}{A} \right\}, \tag{2}$$

where the sum is taken only at points within each box in which $\tilde{q}_y < 0$, Δx and Δy are 1.125° longitude and latitude, respectively, and A is the area of the box. The above measure would give the same value, for instance, if the field of negative $\tilde{q}_y$ covered the entire box, or shrunk to half the area with twice the magnitude. Because the existence of a region of negative $\tilde{q}_y$ ensures a sign reversal in the meridional PV gradient, the two measures of negative $\tilde{q}_y$ shown in Figs. 5 and 6 will sometimes be referred to collectively as "the strength of the sign reversal."

Figure 5a shows the time variation of both measures of negative $\tilde{q}_y$ for the Caribbean using the 20-day filter. Also shown are the times of formation of tropical depressions in the eastern Pacific. A long-period oscillation is clearly present in the meridional PV gradient. Maxima and minima on the min($\tilde{q}_y$) curve (dark line) occur 32–55 days apart and have considerable amplitude. Maxima and minima in the area-weighted negative $\tilde{q}_y$ occur at virtually the same times, suggesting that robust measures of negative $\tilde{q}_y$ have been obtained.

Figure 5b shows the same fields as Fig. 5a, but determined after applying a filter with a 7-day rather than 20-day cutoff. Although many more disturbances appear, the presence of the long-term oscillation is still visible, especially for the last two periods of strong negative $\tilde{q}_y$. This provides some qualititative evidence of the strength of the long-period anomaly.

Figure 6 shows the low-pass filtered measures of negative $\tilde{q}_y$ for the eastern Pacific. Combined with Fig. 5a, an apparent relationship exists between the strength of the sign reversal of the meridional PV gradient and subsequent tropical cyclogenesis. A strong sign reversal occurs initially in the eastern Pacific in mid-June, followed directly by two tropical cyclone formations. About 5 days later, the maximum sign reversal shifts to the Caribbean. Two tropical cyclones form in the eastern Pacific in the following 10 days. This lag is consistent with the time required for the waves to travel from the Caribbean to the tropical cyclone formation region west

of 100°W. The isolated tropical cyclone in mid-July follows an eastern Pacific sign reversal maximum. The sign reversal again shifts eastward to the Caribbean thereafter, and a cluster of tropical cyclones occurs 10–15 days later. Both regions experience a dramatic weakening of the strength of the sign reversal from mid-August to early September, and tropical cyclogenesis ceases entirely. The Caribbean sign reversal sharply increases in the second week of September, and a cluster of four eastern Pacific tropical cyclones occurs in the following two weeks. Finally, the two early October tropical cyclogenesis events follow the strengthening of an eastern Pacific sign reversal in late September.

Figures 5a and 6 show that each incident of eastern Pacific tropical cyclogenesis can be associated either with a near-simultaneous reversal in the eastern Pacific or a prior upstream sign reversal in the Caribbean. Strong sign reversals in each region are never simultaneous; except for the event in late September, the eastern Pacific sign reversals occur first. The results provide circumstantial support for the mechanism described earlier: that easterly waves grow at the longitudes where the sign reversals occur, resulting in downstream formation of tropical storms.

The fluctuations in Fig. 5a occur on the timescale of the Madden–Julian oscillation (hereafter MJO; Madden and Julian 1971, 1994). Because the MJO moves eastward in this region, the shift with time of the maximum negative $\tilde{q}_y$ from the eastern Pacific to the Caribbean is also consistent with the MJO behavior. Recently Boer (1995) has examined the MJO over several years by using global wavenumber 1 velocity potential at 200 mb. Boer (1995) showed four velocity potential maxima during June–August 1991, but only two of these had large amplitude over the eastern Pacific and Caribbean. These two occurred in mid-June and from about 15–23 July. As a result, the timing of Boer's (1995) results are quite consistent with the first two sign reversals shown in Fig. 5a. Boer's data did not extend into September and thus could not confirm the third event in Fig. 5a. The two MJO events shown by Boer (1995) originated in the western Pacific and propagated eastward, but did not reach maximum amplitude until they reached the Caribbean region. The extension of the MJO so far eastward, and its reaching a maximum far from its origin, are both unusual behaviors (Madden and Julian 1994) that may relate to the existence of an El Niño event during 1991.

It appears that the fluctuations shown in Fig. 5a reflect the presence of the MJO. Because velocity potential maxima are consistent with enhanced convection, Boer's (1995) results suggest a connection between the PV sign reversals in Fig. 5a and the enhancement of convection on the same timescale, as was proposed in section 3. Figure 7 shows low-pass-filtered outgoing longwave radiation (OLR) averaged over the region 7.5°–12.5°N, 70°–75°W. This box is approximately centered on the Lake Maracaibo region. It is apparent that three distinct

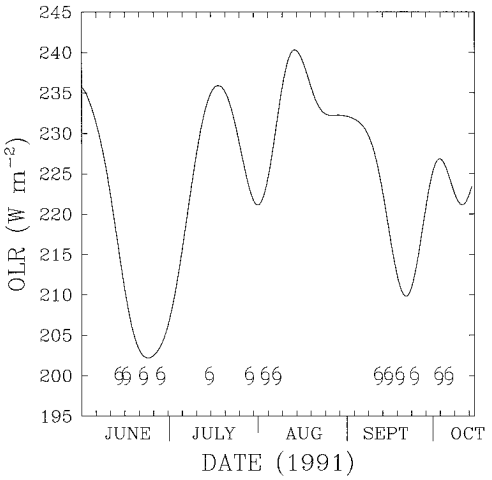

FIG. 7. Outgoing longwave radiation (W m^{-2}), averaged over the region 7.5°–12.5°N, 70°–75°W, and low-pass filtered in the same manner as Fig. 5a.

minima in Caribbean OLR, and thus likely maxima in cumulus convection, occur prior to or during the three clusters of eastern Pacific tropical cyclogenesis. The three convective maxima occur 10 days to 2 weeks after the maximum sign reversals in the Caribbean meridional PV gradient. The timing of these OLR events is unchanged when the averaging area is extended to 2.5°N. It is also unchanged if convective intensity is measured by the (low-pass filtered) number of points in the area that fall below a cutoff value of OLR representative of convection.

Figure 7 provides support from an independent dataset for the existence of the MJO in the region. It also introduces a new question: why the maximum convective heating follows rather than leads the maximum sign reversal in the meridional PV gradient. The reason for this remains uncertain but could relate to an increase in areal coverage of deep convection as a series of synoptic-scale waves intensifies. Recently Chen et al. (1996) showed evidence of such a process occurring in the central Pacific (their Figs. 8i–k), in which a westward-moving synoptic scale wave developed extensive deep convection after forming poleward of an MJO equatorial convective maximum. The synoptic-scale waves are likely to simultaneously act to reduce the background meridional PV gradient by mixing. The combination could produce the time sequence shown in Figs. 5a and 7.

We hypothesize the following sequence of events: (i) the upward motion part of the MJO moves into the eastern Pacific and eventually Caribbean Sea; (ii) enhanced convection with the MJO occurs at 5° and 10°N, but not at 15°N (Gruber 1974); (iii) positive potential vorticity anomalies are enhanced at 10°N over northern South America and along the ITCZ in the eastern Pacific [see idealized modeling results of Schubert et al.

(1991)]; (iv) the consequent PV sign reversal intensifies, allowing easterly waves to form and/or intensify; (v) these waves are the locus of tropical cyclogenesis downstream. This sequence could also provide an explanation for the results of Liebmann et al. (1994), who found that tropical cyclogenesis in the *western* Pacific and Indian Ocean occurred much more frequently during the upward motion phase of the MJO.

5. Discussion

A number of issues have not been addressed in this note that may be relevant for the mechanism proposed here.

1) Evidence has not been provided for wave growth during periods of unstable basic state. Although PV maxima frequently appear between 75° and 85°W in animated loops of PV, spectral analysis does not always show growth of waves of the appropriate frequency. This may not be surprising, given that nonlinear waves will have complicated behavior in the presence of convection and of circulations associated with maintenance of the zonally varying mean jet [see Shapiro (1980) for the latter]. Nevertheless, support for the wave growth hypothesis is provided by the work of Frank (1970). Unlike current practice, Frank (1970) assumed that any easterly waves that could not be tracked with conventional or satellite data had dissipated. Frank found that only about 50% of disturbances reaching Central America in 1969 came from Africa. The remainder developed in the Caribbean between 70° and 85°W, which corresponds quite well to the unstable region in Fig. 2.
2) Shapiro (1980) proposed that vorticity sources, either from those needed to maintain the background state or from convection, could enhance wave growth. For instance, enhanced convection in the ITCZ near northern South America could contribute to wave growth in that region. The relative importance of this mechanism versus that of the unstable basic state noted above has not been determined. The evidence shows, however, that a wave encountering enhanced convective sources of vorticity near South America would also find itself in a region where the Charney–Stern criterion is met, and thus could grow by that process.
3) Attainment of the Charney–Stern instability criterion is not a necessary condition for tropical cyclogenesis. Other mechanisms, such as Zehr's (1992) proposed in situ development from monsoon trough convection, or interactions with upper potential vorticity maxima (Bosart and Bartlo 1991; Montgomery and Farrell 1993), may turn weak preexisting disturbances into tropical cyclones. Nor is the instability a sufficient condition for tropical cyclogenesis; if the sea surface temperature is too low, or perhaps if the vertical shear is too large, a tropical cyclone will likely fail to develop. Rather, the major finding of this work is that the development of a potentially unstable basic state may be the dynamical mechanism by which enhanced ITCZ convection (by whatever cause) is associated with enhanced downstream tropical cyclogenesis.
4) It has been assumed that wave growth in the Caribbean will make eastern Pacific tropical cyclogenesis more likely. Ignored in this assumption is the potentially complex role of the Central American mountains (Zehnder 1993; Zehnder and Gall 1991). Turk et al. (1995) have provided evidence that waves sometimes turn northwestward on the eastern side of the Mexican mountains, followed by surface cyclogenesis west of the mountains and south of the Gulf of Tehuantepec. The evolution strongly resembles the theory proposed by Zehnder and Gall (1991). During other times, the waves appeared to cross from the Atlantic to the Pacific at a lower latitude with much less mountain interaction. A complete understanding of the role of Caribbean PV gradients in eastern Pacific cyclogenesis will require knowledge of the role of mountains.
5) As noted in the introduction, many researchers and operational forecasters believe that eastern Pacific tropical cyclones develop almost exclusively in association with synoptic-scale waves that themselves originate in Africa (Avila and Pasch 1992; P. Black 1996, personal communication). Bister and Emanuel (1997) describe the significance of mesoscale moisture variation during an eastern Pacific tropical cyclone genesis (Hurricane Guillermo) in 1991. Nevertheless, they note the existence of a westward-propagating synoptic-scale easterly wave in the western Caribbean prior to cyclogenesis.

   Alternatively, Ferreira and Schubert (1997) proposed that the Charney–Stern instability created by ITCZ heating can produce breakdown of the ITCZ into disturbances that eventually become tropical cyclones, without need for a preexisting upstream easterly wave. The two-stage mechanism of Zehr (1992) requires neither a dynamically unstable basic state nor a synoptic-scale wave in the easterlies.

   The evidence from this work suggests indirectly that upstream wave growth plays a role. The proposed mechanism allows but does not require an African wave precursor. It is apparent from this study and from those noted above that the origin and formation mechanism(s) of eastern Pacific tropical cyclones remain uncertain.

Nevertheless, some unambiguous conclusions can be made from the results presented here. First, a strong zonal variation in basic-state potential vorticity existed in the Atlantic and Caribbean basins in the layer encompassing isentropic surfaces from 310 to 320 K during the summer of 1991. Its major feature was a large region of sign reversal of the meridional potential vor-

ticity gradient in the Caribbean Sea. This zonal inhomogeneity likely had a substantial impact on the behavior of easterly waves. Second, an apparent relationship existed in 1991 between the strength of the negative meridional PV gradient in the Caribbean and subsequent downstream development of tropical cyclones in the eastern Pacific. Furthermore, the evolution of the meridional potential vorticity gradient appeared to be associated with the Madden–Julian oscillation. It has been hypothesized that it is the growth of waves on an unstable basic state that provides the connection between the MJO and the associated enhanced tropical cyclogenesis.

Only one season of data was presented here. Other seasons and other ocean basins must be investigated to see whether the correlation between upstream meridional PV gradient and tropical cyclogenesis commonly occurs. This work is under way and will be reported on at a later time.

Acknowledgments. One of us (JM) has had enlightening conversations about wave propagation and other aspects of this work with David Raymond of New Mexico Tech and Kerry Emanuel of MIT. We have also had beneficial discussions with Lloyd Shapiro of the Hurricane Research Division of NOAA (HRD) and Arthur Loesch and Daniel Keyser of the SUNY/Albany Department of Atmospheric Science. Peter Black of HRD first proposed the eastern Pacific MJO connection during the TEXMEX data collection effort in 1991. We thank Gary Lackmann (now at McGill University) and Daniel Keyser for the computer code for the Lanczos filter. We are indebted to Richard Pasch of the National Hurricane Center for providing information on eastern Pacific tropical depressions 5 and 10 of 1991. Finally, we thank Anton Seimon, not only for locating the references about the ''Relampago del Catatumbo,'' but also for providing translations from the Spanish.

The gridded analyses for this study were generated by the European Centre for Medium-Range Weather Forecasts. Most were obtained directly from ECMWF; the remainder were accessed via the National Center for Atmospheric Research (NCAR), which is funded by the National Science Foundation. The OLR data were also acquired from archives at NCAR. This study was supported by National Science Foundation Grant 9529771 and by Office for Naval Research Grant N00014-94-I-0289.

REFERENCES

Avila, L. A., 1991: Eastern North Pacific hurricane season of 1990. *Mon. Wea. Rev.,* **119,** 2034–2046.

——, and R. J. Pasch, 1992: Atlantic tropical systems of 1991. *Mon. Wea. Rev.,* **120,** 2688–2696.

Betts, A. K., 1975: Parametric interpretation of trade wind cumulus budget studies. *J. Atmos. Sci.,* **32,** 1934–1945.

Bister, M., and K. A. Emanuel, 1997: The genesis of Hurricane Guillermo: TEXMEX analyses and a modeling study. *Mon. Wea. Rev.,* **125,** 2662–2682.

Boer, G. J., 1995: Analyzed and forecast large-scale tropical divergent flow. *Mon. Wea. Rev.,* **123,** 3539–3553.

Bosart, L. F., and J. A. Bartlo, 1991: Tropical storm formation in a baroclinic environment. *Mon. Wea. Rev.,* **119,** 1979–2013.

Burpee, R. W., 1972: The origin and structure of easterly waves in the lower troposphere of North Africa. *J. Atmos. Sci.,* **29,** 77–90.

Carlson, T. N., 1969: Some remarks on African disturbances and their progress over the tropical Atlantic. *Mon. Wea. Rev.,* **97,** 716–726.

Charney, J. G., and M. E. Stern, 1962: On the stability of internal baroclinic jets in a rotating atmosphere. *J. Atmos. Sci.,* **19,** 159–172.

Chen, S. S., R. A. Houze, and B. E. Mapes, 1996: Multiscale variability of deep convection in relation to large-scale circulation in TOGA COARE. *J. Atmos. Sci.,* **53,** 1380–1409.

Codazzi, A., 1841: *Resumen de la Geografia de Venezuela*. Reprinted 1940, R. M. Baralt and R. Diaz, Eds., Taller de Artes Graficas, Escuela Tecnica Industrial, 303 pp. [Available from State University of New York at Albany, 1400 Washington Avenue, Albany, NY 12222.]

Duchon, C. E., 1979: Lanczos filtering in one and two dimensions. *J. Appl. Meteor.,* **18,** 1016–1022.

Eliassen, A., 1983: The Charney–Stern theorem on barotropic–baroclinic instability. *Pure Appl. Geophys.,* **121,** 563–573.

Ferreira, R. N., and W. H. Schubert, 1997: Barotropic aspects of ITCZ breakdown. *J. Atmos. Sci.,* **54,** 261–285.

Fjörtoff, R., 1950: Application of integral theorems in deriving criteria of stability for laminar flows and for the baroclinic circular vortex. *Geofis. Publ.,* **17**(6), 1–52.

Frank, N. L., 1970: Atlantic tropical systems of 1969. *Mon. Wea. Rev.,* **98,** 307–314.

Gruber, A., 1974: Wavenumber–frequency spectra of satellite-measured brightness in the tropics. *J. Atmos. Sci.,* **31,** 1675–1680.

——, and A. F. Krueger, 1984: The status of the NOAA outgoing longwave radiation data set. *Bull. Amer. Meteor. Soc.,* **65,** 958–962.

Haynes, P. H., and M. E. McIntyre, 1987: On the evolution of vorticity and potential vorticity in the presence of diabatic heating and frictional or other forces. *J. Atmos. Sci.,* **44,** 828–841.

Hendon, H. H., 1986: Streamfunction and velocity potential representation of equatorially trapped waves. *J. Atmos. Sci.,* **43,** 3038–3042.

Krishnamurti, T. N., C. E. Levy, and H.-L. Pan, 1975: On simultaneous surges in the trades. *J. Atmos. Sci.,* **32,** 2367–2370.

Lanczos, C., 1956: *Applied Analysis.* Prentice-Hall, 539 pp.

Liebmann, B., and H. H. Hendon, 1990: Synoptic-scale disturbances near the equator. *J. Atmos. Sci.,* **47,** 1463–1479.

——, ——, and J. D. Glick, 1994: The relationship between tropical cyclones of the western Pacific and Indian Oceans and the Madden–Julian oscillation. *J. Meteor. Soc. Japan,* **72,** 401–411.

Madden, R. A., and P. R. Julian, 1971: Description of a 40–50 day oscillation in the zonal wind in the tropical Pacific. *J. Atmos. Sci.,* **28,** 702–708.

——, and ——, 1994: Observations of the 40–50 day tropical oscillation—A review. *Mon. Wea. Rev.,* **122,** 814–837.

Molinari, J., S. Skubis, and D. Vollaro, 1995: External influences on hurricane intensity. Part III: Potential vorticity evolution. *J. Atmos. Sci.,* **52,** 3593–3606.

Montgomery, M. T., and B. F. Farrell, 1993: Tropical cyclone formation. *J. Atmos. Sci.,* **50,** 285–310.

Nakazawa, T., 1986: Intraseasonal variations of OLR in the tropics during the FGGE year. *J. Meteor. Soc. Japan,* **64,** 17–33.

Nitta, T., and S. Esbensen, 1974: Heat and moisture budget analyses using BOMEX data. *Mon. Wea. Rev.,* **102,** 17–28.

——, and Y. Takabayu, 1985: Global analysis of the lower tropospheric disturbances in the tropics during the northern summer

of the FGGE year. Part II: Regional characteristics of the disturbances. *Pure Appl. Geophys.,* **123,** 272–292.

Rappaport, E. N., and M. Mayfield, 1992: Eastern North Pacific hurricane season of 1991. *Mon. Wea. Rev.,* **120,** 2697–2708.

Reed, R. J., A. Hollingsworth, W. A. Heckley, and F. Delsol, 1988: An evaluation of the performance of the ECMWF operational system in analyzing and forecasting easterly wave disturbances over Africa and the tropical Atlantic. *Mon. Wea. Rev.,* **116,** 824–865.

Schubert, W. H., P. E. Ciesielski, D. E. Stevens, and H. Kuo, 1991: Potential vorticity modeling of the ITCZ and the Hadley circulation. *J. Atmos. Sci.,* **48,** 1493–1509.

Shapiro, L. J., 1977: Tropical storm formation from easterly waves: A criterion for development. *J. Atmos. Sci.,* **34,** 1007–1021.

——, 1980: The effect of nonlinearities on the evolution of barotropic easterly waves in a non-uniform environment. *J. Atmos. Sci.,* **37,** 2631–2643.

——, 1986: The three-dimensional structure of synoptic-scale disturbances over the tropical Atlantic. *Mon. Wea. Rev.,* **114,** 1876–1891.

Thorncroft, C. D., and B. J. Hoskins, 1994a: An idealized study of African easterly waves. Part I: A linear view. *Quart. J. Roy. Meteor. Soc.,* **120,** 953–982.

——, and ——, 1994b: An idealized study of African easterly waves. Part II: A nonlinear view. *Quart. J. Roy. Meteor. Soc.,* **120,** 983–1016.

Turk, M., D. Vollaro, and J. Molinari, 1995: Large-scale aspects of active and inactive periods of eastern Pacific tropical cyclogenesis. Preprints, *21st Conf. on Hurricanes and Tropical Meteorology,* Miami, FL, Amer. Meteor. Soc., 106–107.

Zehnder, J. A., 1993: The influence of large-scale topography on barotropic vortex motion. *J. Atmos. Sci.,* **50,** 2519–2532.

——, and R. L. Gall, 1991: On a mechanism for orographic triggering of tropical cyclones in the eastern North Pacific. *Tellus,* **43A,** 25–36.

Zehr, R. M., 1992: Tropical cyclogenesis in the western north Pacific. NOAA Tech. Rep. NESDIS 61, 181 pp. [Available from the National Technical Information Service, U.S. Department of Commerce, Sills Bldg., 5285 Port Royal Road, Springfield, VA 22161.]